Aquaporin 5-deficient mouse lungs are hyperresponsive to cholinergic stimulation

Carissa M. Krane*, Christopher N. Fortner†, Arthur R. Hand‡, Dennis W. McGraw§, John N. Lorenz†, Susan E. Wert¶, Jennifer E. Towne*, Richard J. Paul†, Jeffrey A. Whitsett¶, and Anil G. Menon*‖

Departments of *Molecular Genetics, Biochemistry, and Microbiology, †Molecular and Cellular Physiology, and §Medicine, University of Cincinnati College of Medicine, Cincinnati, OH 45267-0524; ‡Department of Pediatric Dentistry, University of Connecticut Health Center, School of Dental Medicine, Farmington, CT 06030; and ¶Division of Pulmonary Biology, Children's Hospital Medical Center, Cincinnati, OH 45229

Edited by Peter C. Agre, Johns Hopkins University School of Medicine, Baltimore, MD, and approved September 7, 2001 (received for review May 31, 2001)

Although aquaporin 5 (AQP5) is the major water channel expressed in alveolar type I cells in the lung, its actual role in the lung is a matter of considerable speculation. By using immunohistochemical staining, we show that AQP5 expression in mouse lung is not restricted to type I cells, but is also detected in alveolar type II cells, and in tracheal and bronchial epithelium. *Aqp5* knockout (*Aqp5*$^{-/-}$) mice were used to analyze AQP5 function in pulmonary physiology. Compared with *Aqp5*$^{+/+}$ mice, *Aqp5*$^{-/-}$ mice show a significantly increased concentration-dependent bronchoconstriction to intravenously administered Ach, as shown by an increase in total lung resistance and a decrease in dynamic lung compliance ($P < 0.05$). Likewise, Penh, a measure of bronchoconstriction, was significantly enhanced in *Aqp5*$^{-/-}$ mice challenged with aerosolized methacholine ($P < 0.05$). The hyperreactivity to bronchoconstriction observed in the *Aqp5*$^{-/-}$ mice was not due to differences in tracheal smooth muscle contractility in isolated preparations or to altered levels of surfactant protein B. These data suggest a novel pathway by which AQP5 influences bronchoconstriction. This observation is of special interest because studies to identify genetic loci involved in airway hyperresponsiveness associated with asthma bracket genetic intervals on human chromosome 12q and mouse chromosome 15, which contain the *Aqp5* gene.

Aquaporin 5 (AQP5) is a mercury-sensitive water channel expressed in mouse salivary gland acinar cells, alveolar type I cells, lacrimal glands, and the eye (1–3). However, the function of AQP5 in mouse lung physiology and pathophysiology is largely unknown. Recent studies have explored the regulation of *Aqp5* gene expression in normal and disease states. In a mouse model of acute lung injury, AQP5 mRNA and protein expression were significantly decreased in association with pulmonary inflammation and edema resulting from adenoviral infection (4). Moreover, AQP5 expression in a murine lung epithelial cell line (MLE-12) is modulated by the proinflammatory cytokine TNF-α through an nuclear factor (NF)-κB-dependent pathway (5). Keratinocyte growth factor also has been shown to mediate the differentiation status of alveolar epithelial cells and AQP5 expression (6). However, a clear understanding of AQP5 function in the lung remains to be discerned.

Previously published studies have addressed functional questions limited to the examination of the role of AQP5 in type I cells in fluid clearance and airspace-capillary osmotic water permeability. Of significance, isolated perfused lungs from *Aqp5*$^{-/-}$ mice were shown to have a 10-fold reduction in airspace-capillary osmotic water permeability (7). Experiments addressing the role of AQP5 in alveolar fluid clearance failed to indicate a role for AQP5 in this process under certain physiological conditions (8). Based on the results of these studies, some have concluded that AQP5 does not play a major role in lung physiology. Contrary to these conclusions, the data reported here clearly define a novel function for AQP5 in lung physiology.

In this report, we have examined the expression pattern of AQP5 in the lung and have shown that, in addition to expression in alveolar type I cells, AQP5 is also detected in alveolar type II cells and tracheal and bronchial epithelium in mice. By using *Aqp5*$^{-/-}$ mice, we have directly assessed AQP5 function in the lung by using histological and physiological analyses. Our results show a novel role for AQP5 in airway responsiveness. Interestingly, previously reported genetic linkage studies identify syntenic regions of mouse chromosome 15 (9) and human chromosome 12q (10, 11), in which Aqp5 resides (12, 13), as containing loci linked with hyperreactivity to bronchoconstriction. This genetic evidence supports the physiological results presented here, which implicate AQP5 in the pathogenesis of bronchial hyperreactivity.

Methods

Aqp5-Deficient Mice. Mice null for *Aqp5* were generated as described (14). Mice were bred and housed in a pathogen-free environment. Age- and sex-matched 12-week-old *Aqp5*$^{+/+}$ and *Aqp5*$^{-/-}$ littermates (F_4 generation) from *Aqp5* recombinant inbred 129SvJ/Black Swiss (line 187) were used in all experiments. All experiments involving the use of live mice were approved by the Institutional Animal Care and Use Committee review board of the University of Cincinnati College of Medicine.

Histology and Immunohistochemistry. Mouse lungs from 12-week-old sex-matched *Aqp5*$^{+/+}$ and *Aqp5*$^{-/-}$ littermates were inflation-fixed in phosphate buffered 4% paraformaldehyde, paraffin-embedded, and sectioned at 5 μm. Immunohistochemical staining was evaluated as described (4), by using a peptide-derived, monospecific rabbit polyclonal antibody raised against the mouse/rat AQP5 C-terminal peptide sequence (LL639; 0.5 μg/ml; ref. 13) and a Vectastain ABC Peroxidase Elite Anti-Rabbit IgG kit (Vector Laboratories, Burlingame, CA) to detect the antigen:antibody complexes. Briefly, inflation-fixed lungs were washed in PBS and paraffin embedded. Paraffin-embedded lungs were section at 5 μm and deparaffinized in Hemo-De (Fisher Scientific), followed by ethanol rehydration. Slides were placed in methanol containing 0.5% hydrogen peroxide for the removal of endogenous peroxidase activity. Nonspecific binding was blocked by incubation of the sections in 0.1 M PBS (pH 7.4), containing 0.2% Triton X-100 and 2% normal goat serum at room temperature for 1 h. Lung sections were incubated with peptide-derived polyclonal antibody raised against mouse/rat AQP5 C-terminal peptide residues (LL639; 0.5 μg/ml; ref. 13) overnight at 4°C. Sections were rinsed five times in 0.1 M

This paper was submitted directly (Track II) to the PNAS office.

Abbreviations: AQP, aquaporin; R_T, total lung resistance; C_{dyn}, dynamic lung compliance; APTI, airway pressure-time index; Ach, acetylcholine; SP-B, surfactant protein B; Penh, enhanced pause.

‖To whom reprint requests should be addressed at: University of Cincinnati College of Medicine, Department of Molecular Genetics, Biochemistry and Microbiology, 231 Albert Sabin Way, Cincinnati, OH 45267-0524. E-mail: anil.menon@uc.edu.

The publication costs of this article were defrayed in part by page charge payment. This article must therefore be hereby marked "*advertisement*" in accordance with 18 U.S.C. §1734 solely to indicate this fact.

www.pnas.org/cgi/doi/10.1073/pnas.231273398

PBS-0.2% Triton X-100 and incubated for 1 h at room temperature with biotinylated goat anti-rabbit secondary antibody (Vector Laboratories), followed by incubation with an avidin-biotin complex (Vector Laboratories) for 1 h at room temperature. Sections were washed with PBS, rinsed in 0.1 M acetate buffer (pH 6.0), and incubated with NiDAB in 0.1 M acetate buffer (pH 6.0) for 4 min, rinsed, in Tris Buffer (pH 7.6) and incubated in Tris-cobalt for 4 min, rinsed, and counterstained with Nuclear Fast Red (Vector Laboratories). Labeling controls were performed under the same conditions and included the following: (*i*) substitution of the primary antibody with preimmune rabbit immunoglobulin G purified on a protein A column (Pierce); (*ii*) omission of either the primary or secondary antibody to check for endogenous biotin and peroxidase activity, as well as nonspecific binding of the secondary antibody; and (*iii*) preincubation of the primary antibody with an excess of the immunizing peptide (4, 13).

Electron Microscopy. Mouse lungs were inflation-fixed with 2.5% glutaraldehyde in 0.1 M sodium cacodylate buffer (pH 7.4), for morphological analyses, or with 3% paraformaldehyde-0.1% glutaraldehyde in 0.1 M cacodylate buffer (pH 7.4), for immunogold labeling. Subsequent processing, embedding, sectioning, and labeling procedures were carried out as previously described (15). Sections were examined and photographed at 60 kV in a Philips CM10 TEM.

Wet-to-Dry Weight Ratios. Wet-to-dry weight ratios were determined for lung tissue excised from $Aqp5^{+/+}$ and $Aqp5^{-/-}$ mice ($n = 8$ each group) as described (4).

Gas Exchange. Lung CO_2 exchange was analyzed in anesthetized, mechanically ventilated $Aqp5^{+/+}$ and $Aqp5^{-/-}$ mice ($n = 6$ each group) as described (16). Mice were first ventilated with 95% O_2/5% CO_2 for 10 min, and two 40-μl arterial blood samples were taken via a carotid catheter to establish a baseline. Mice were then ventilated with 100% O_2, and arterial blood samples were taken at 30 s, 3 min, 6 min, and 9 min under this condition. Arterial pCO_2, pO_2, and pH were analyzed by using a Chiron (Norwood, MA) blood gas analyzer (model 384).

Resistance and Compliance Measurements. Pulmonary responsiveness to bronchoconstrictor agents was determined by measuring airway pressure and flow in anesthetized, ventilated $Aqp5^{+/+}$ and $Aqp5^{-/-}$ mice ($n = 6$ each group) according to a published method (17). Briefly, anesthetized mice were tracheostomized by using a custom built cannula with ports for inspiration and expiration, and for monitoring airway pressure and airway flow. The femoral artery and vein were cannulated for continuous monitoring of blood pressure and the i.v. administration of drugs. Ventilation and data collection and analysis were accomplished by using a custom written software program (Mouse Reactivity System, U.S. Environmental Protection Agency, Research Triangle Park, NC), which uses flow and pressure signals to calculate total lung resistance (R_T) and dynamic compliance (C_{dyn}). In addition, the airway pressure-time index (APTI) was calculated by integrating the change in peak airway pressure for the 2-min period after administration of each challenge dose, as previously described (18). Mice were ventilated at a rate of 150 breaths per minute and a tidal volume of $\approx$200 μl. Values from each breathing cycle were averaged over 2-s intervals and saved to a data file. After establishing a baseline, mice were challenged with increasing doses of Ach administered i.v. via a jugular catheter (1–1,000 ng/g body weight, delivered in a 10 μl bolus of saline). Four to eight minutes were allowed between doses to permit a return to baseline values.

Whole Animal Barometric Plethysmography. Airway responsiveness to methacholine was determined in awake, unrestrained $Aqp5^{+/+}$ and $Aqp5^{-/-}$ mice ($n = 6$ each group) by using barometric plethysmography to measure enhanced pause (Penh), a unitless measure that has been shown to correlate with the changes in airway resistance that occur during bronchial challenge with methacholine (19). Mice were equilibrated in the plethysmography chamber for 10 min before challenge. By using a previously reported protocol (20), mice were challenged with increasing doses of methacholine (2.5 mg/ml to 80 mg/ml) after baseline Penh was first established with aerosolized PBS. Each dose was delivered over 1 min, and Penh was recorded continuously for 4 min afterward. Data for each mouse were analyzed and plotted by using GraphPad PRISM software.

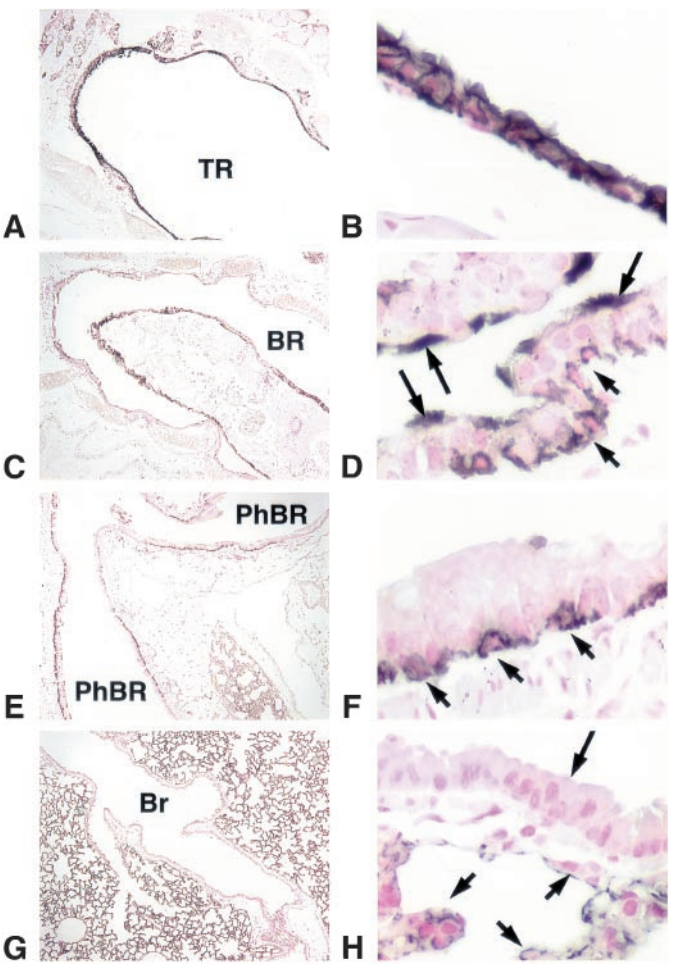

Fig. 1. Immunohistochemical localization of AQP5 in mouse airway epithelium. AQP5 expression (black reaction product) was observed in epithelial cells of the trachea (*A* and *B*), of the right and left main stem bronchi (illustrated here, where these structures arise at the carina tracheae) (*C* and *D*), and in the perihilar regions of the proximal, extrapulmonary, lobar bronchi (*E* and *F*), but not in the more distal intrapulmonary bronchioles (*G* and *H*). Positive immunostaining of both secretory and ciliated cells of the trachea is shown at a higher magnification in *B*. Evidence for positive immunostaining of basal (arrowheads) and ciliated (arrows) cells located in the main stem bronchi is shown in *D* at a higher magnification. In the epithelium of the perihilar, lobar bronchioles, AQP5 expression was restricted to basal cells (arrowheads) as shown in *F*. No immunostaining was found in the epithelial cells of the intrapulmonary bronchioles (arrows), although positive immunostaining for AQP5 was detected along the luminal surface of the alveolar epithelium (arrowheads) in *H*. Original magnification of *A*, *C*, *E*, and *G* = ×5; magnification of *B*, *D*, *F*, and *H* = ×80. TR, trachea; BR, mainstem bronchi; PhBR, perihilar bronchioles; Br, bronchioles.

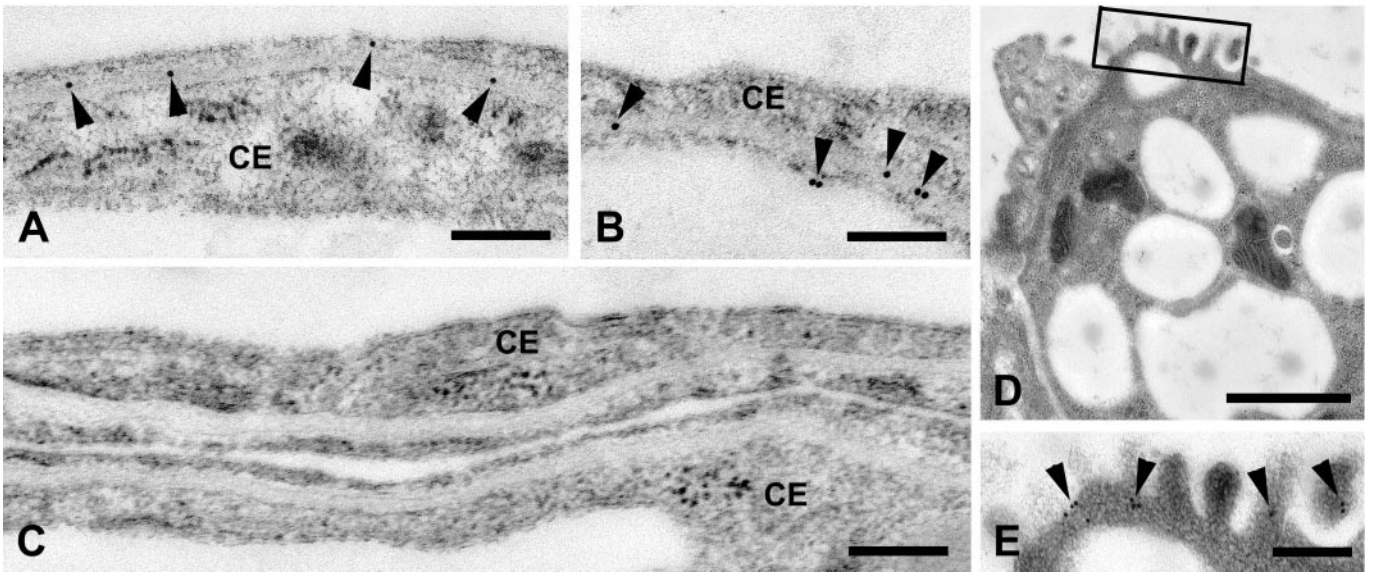

Fig. 2. Immunogold localization of AQP5 in the distal mouse lung. Thin sections of LR Gold embedded lung tissue from $Aqp5^{+/+}$ and $Aqp5^{-/-}$ mice were incubated with anti-AQP5 antibody (diluted 1:30) overnight at 4°C. Bound antibody was subsequently visualized with goat anti-rabbit IgG labeled with 10 nm gold particles (Amersham Pharmacia). (*A* and *B*.) Portions of alveolar septa of $Aqp5^{+/+}$ mice showing AQP5 labeling in type I cells; gold particles (arrowheads) appear to be associated with both the apical and basal surfaces of the thin epithelial cells. The capillary endothelium (CE) is unreactive (bars = 0.25 μm). (*C*) Identical concentration of anti-AQP5 antibody incubated with a distal lung section from an $Aqp5^{-/-}$ mouse; the type I cells lining the collapsed alveolus (between the two endothelial cells, CE) are unlabeled (bar = 0.25 μm). (*D*) Alveolar type II cell of $Aqp5^{+/+}$ mouse; without osmium postfixation, the lamellar bodies are electron lucent (bar = 1 μm). (*E*) Higher magnification of *D* showing AQP5 labeling of the apical microvilli of the type II cell (bar = 0.25 μm).

Tracheal Smooth Muscle Contraction. Isometric force measurements of tracheal smooth muscle contractility were determined in isolated tracheal ring preparations from $Aqp5^{+/+}$ and $Aqp5^{-/-}$ mice ($n = 6$ each group) as described (21). Cumulative concentration force relationships to Ach (10^{-8}–10^{-4} M), and relaxation to isoproterenol (10^{-9}–10^{-5} M), after a precontraction with 10^{-5} M Ach. Epithelial-dependent relaxation to substance P (10^{-9} M) or ATP (10^{-5} M) also were assessed.

Surfactant Protein B (SP-B) ELISA. SP-B concentrations were determined from bronchoalveolar lavage or total lung homogenates from $Aqp5^{+/+}$ and $Aqp5^{-/-}$ mice ($n = 6$ each group) as described (22). SP-B concentration was expressed as ng/ml of bronchoalveolar lavage fluid and as ng SP-B/mg protein. Values represent the mean value ± SE.

Results

AQP5 Expression in Mouse Lung. By using immunohistochemical staining and light microscopy, AQP5 expression was previously reported in alveolar Type I cells of the mouse lung (2), and in rat distal lung, perihilar region of the conducting airway, and nasopharynx (1, 3). In humans, *in situ* hybridization and immunofluorescence were previously used to detect AQP5 expression in the apical membrane of columnar cells of the superficial epithelium and submucosal gland acinar cells of nose and bronchial epithelia, and alveolar Type I cells (23). Our data show that, in addition to alveolar Type I cell expression, immunohistochemical staining of lung sections from $Aqp5^{+/+}$ mice showed AQP5 immunoreactivity in epithelial cells of the trachea, main stem bronchi, and extrapulmonary lobar bronchioles, but not in the bronchiolar epithelium of the more distal, intrapulmonary bronchioles (Fig. 1). In the trachea, immunopositive staining for AQP5 was detected at the apical, basal, and basal-lateral surfaces of both secretory and ciliated epithelial cells (Fig. 1 *A* and *B*). In the main stem bronchi, immunopositive staining was detected in cells located along the basal aspect of the bronchial epithelium, as well as along the luminal surface in association with ciliated cells (Fig. 1 *C* and *D*). In the perihilar region of the lobar bronchioles, immunopositive staining was restricted to cells located along the basal aspect of the epithelium (Fig. 1 *E* and *F*). Although no immunostaining was detected in the intrapulmonary bronchioles, staining was detected along the apical, or luminal, surface of the alveolar epithelium (Fig. 1 *G* and *H*). No immunoreactivity was observed in wild-type sections incubated with primary antibody preabsorbed with the immunizing peptide, with preimmune serum, or with secondary antibody only controls (4). Likewise, no immunoreactivity was seen in lung sections from $Aqp5^{-/-}$ mice reacted with the AQP5 antibody (data not shown).

Immunogold labeling of thin sections of the distal lung with anti-AQP5 antibodies revealed expression of AQP5 in alveolar type I (Fig. 2 *A* and *B*) and alveolar type II cells (Fig. 2 *D* and *E*). In type I cells, gold particles were associated with both the apical and basal cell membranes. In type II cells, labeling of the microvilli on the apical cell membrane was most prominent. No immunospecific staining was observed in lungs from $Aqp5^{-/-}$ mice (Fig. 2*C*).

Wet-to-Dry Weight. In addition to microscopic evaluation, wet-to-dry weight ratios were used to assess potential pulmonary edema and/or fluid imbalance in lungs from *Aqp5* null mice (data not shown). No significant difference was observed between the two genotypes, suggesting that, under normal physiological conditions, AQP5 deficiency does not cause pulmonary edema.

Gas Exchange. Because AQP5 is expressed in the alveolar epithelium at the site of gas exchange, $Aqp5^{+/+}$ and $Aqp5^{-/-}$ mice were analyzed for the ability to transport gases via arterial blood exchange. Arterial blood O_2, CO_2, and pH were assessed under conditions of 95% O_2/5% CO_2, and at 30 s, 3 min, 6 min, and 9 min after a switch to 100% O_2. No significant differences were observed between the two genotypes (data not shown), suggesting that, under normal conditions, AQP5 deficiency does not result in an altered ability to effectively exchange gases.

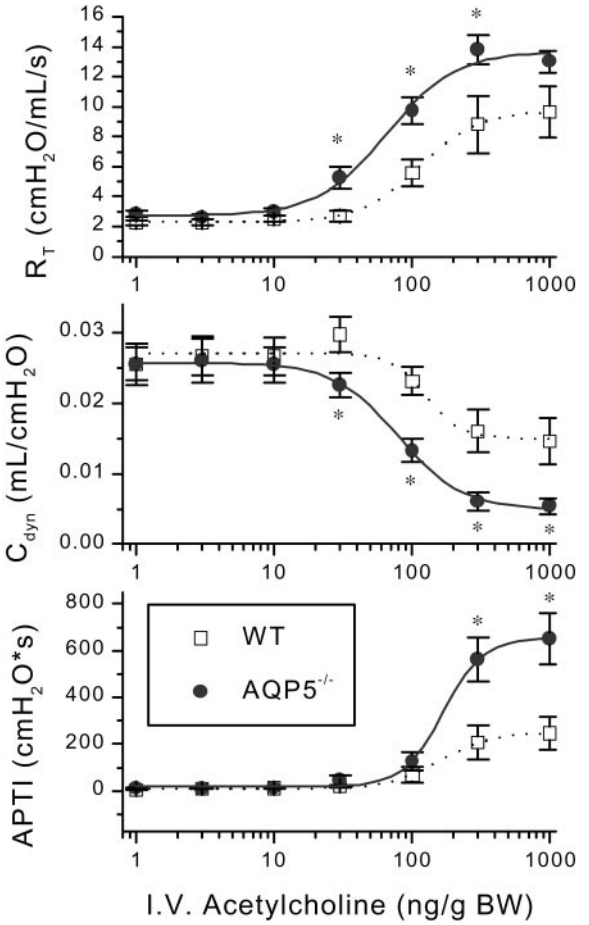

Fig. 3. Airway responsiveness of *Aqp5*$^{+/+}$ and *Aqp5*$^{-/-}$ mice to i.v. bronchoconstricton. Total pulmonary resistance (R_T) (*A* and *D*), dynamic compliance (C_{dyn}) (*B* and *E*), and airway pressure time index (APTI) (*C* and *F*) were measured and computed for anesthetized mechanically ventilated *Aqp5*$^{+/+}$ vs. *Aqp5*$^{-/-}$ mice in response to i.v. brochoconstrictor challenge with ACh (*A–C*) or U46619 (*D–F*). A dose-response curve was generated with sequential challenge of increasing doses of agonist (see *Methods*). *Aqp5*$^{-/-}$ (filled circle, solid line) mice were hyperreactive to bronchoconstriction with ACh as compared with *Aqp5*$^{+/+}$ (open square, dotted line) littermate controls. Values are means ± SE; *, $P < 0.05$ compared with *Aqp5*$^{+/+}$.

Airway Responsiveness. AQP5 expression in the conducting airways suggests a role for AQP5 in regulating pulmonary mechanics. Airway reactivity was evaluated by measuring total lung resistance (R_T) and dynamic compliance (C_{dyn}), as well as the APTI in anesthetized, ventilated mice (Fig. 3 *A–C*). *Aqp5*$^{-/-}$ mice were found to be hyperreactive to intravenously administered ACh (Fig. 3 *A–C*) as compared with wild-type littermates. Although there were no differences in the baseline measurements of R_T and C_{dyn} between the two groups of animals, the magnitude of the responses of both variables to increasing doses of ACh was increased in *Aqp5* $^{-/-}$ mice compared with *Aqp5*$^{+/+}$ mice ($P < 0.05$). Furthermore, the APTI response to ACh, which is a measure of not only the peak magnitude but also the duration of the constrictor response, was markedly increased in the *Aqp5*$^{-/-}$ mice.

Whole body barometric plethysmography was used to determine whether hyperreactivity to bronchoconstriction could be induced via inhalation of methacholine in awake, unrestrained, spontaneously breathing *Aqp5* null mice. In this method, the enhanced pause (Penh) was used as a measure of bronchoconstriction (see *Methods*). Consistent with the resistance and

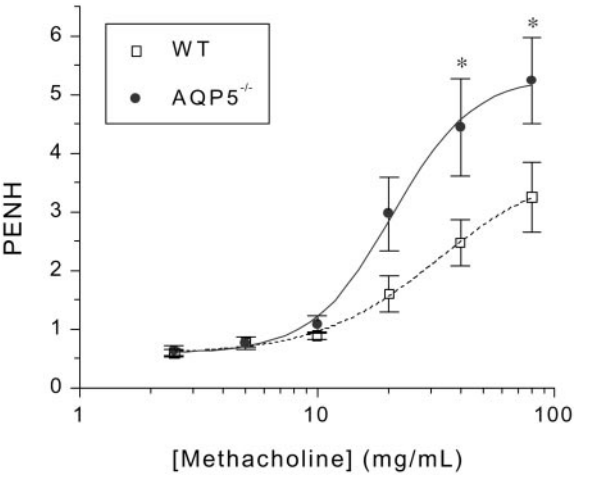

Fig. 4. Airway responsiveness of *Aqp5*$^{+/+}$ and *Aqp5*$^{-/-}$ mice to bronchoconstriction by inhaled methacholine. Penh was used as a measure of bronchoconstriction in whole body plethysmography of awake, unrestrained mice in response to inhaled methacholine. A dose-response curve was generated with sequential challenge of increasing concentrations of agonist (see *Methods*). *Aqp5*$^{-/-}$ (filled circle, solid line) mice were hyperreactive to bronchoconstriction with methacholine as compared with *Aqp5*$^{+/+}$ (open square, dotted line) littermate controls. Values are means ± SE; *, $P < 0.05$ compared with *Aqp5*$^{+/+}$ ($n = 6$ each group).

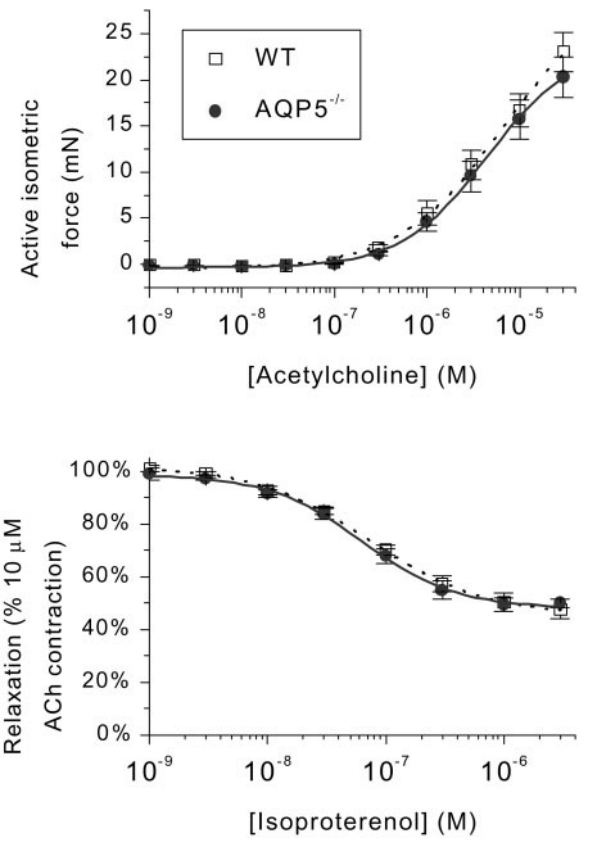

Fig. 5. Isometric force measurements for isolated tracheal rings from *Aqp5*$^{+/+}$ and *Aqp5*$^{-/-}$ mice. Tracheal smooth muscle (*A*) contraction to ACh, expressed as milli-Newtons (mN) and (*B*) relaxation to isoproterenol are expressed as a percentage of the constriction to 10^{-5} M ACh (see *Methods*). No statistically significant differences were observed between *Aqp5*$^{+/+}$ (open square, dotted line) vs. *Aqp5*$^{-/-}$ (filled circle, solid line) tracheas. In addition, no difference in relaxation was observed with either substance P or ATP (not shown). Values are means ± SE ($n = 6$ each group)

PHYSIOLOGY

compliance results compiled by using ACh as an agonist, $Aqp5^{-/-}$ mice were hyperreactive to bronchoconstriction by inhaled methacholine in a dosage-dependent fashion (Fig. 4). Thus, AQP5 deficiency results in airway hyperreactivity to bronchoconstriction with cholinergic stimulation, independent of the route of administration.

Isometric Force Measurements of Tracheal Smooth Muscle. Although AQP5 expression is restricted to epithelial cells in the lung, we wanted to rule out whether the effect of cholinergic stimulation on bronchoconstriction in the absence of AQP5 expression was mediated by a difference in tracheal smooth muscle contractility. Isometric force measurements were analyzed by using isolated tracheal rings from $Aqp5^{+/+}$ and $Aqp5^{-/-}$ mice. No significant difference in ACh-induced contractility (Fig. 5*A*) or isoproterenol-induced relaxation (after ACh-induced contraction; Fig. 5*B*) was observed between the tracheas from $Aqp5^{+/+}$ or $Aqp5^{-/-}$ mice, suggesting that tracheal smooth muscle contractility was not affected by AQP5 deficiency. Epithelial-dependent relaxation to SP or ATP also was not affected (data not shown).

Surfactant Protein-B (SP-B). SP-B is a 79-aa polypeptide expressed in alveolar type II cells that interacts with phospholipids to enhance the surface tension of the alveolus in the lung (24). Deficiency in SP-B has been shown to affect lung function, and results in reduced lung compliance (25). SP-B concentrations were analyzed from total lung homogenates and bronchoalveolar lavages from $Aqp5^{+/+}$ and $Aqp5^{-/-}$ mice. No significant differences were observed in SP-B concentrations obtained from lung homogenates ($Aqp5^{+/+}$: 15.4 $\pm$ 1.46 ng SP-B/mg protein; $Aqp5^{-/-}$: 14.6 $\pm$ 1.42 ng SP-B/mg protein) or from lung lavages ($Aqp5^{+/+}$: 262 $\pm$ 25.7 ng SP-B/ml lavage fluid; $Aqp5^{-/-}$: 264 $\pm$ 25.01 ng SP-B/ml lavage fluid), suggesting that AQP5 deficiency did not result in altered SP-B concentration.

Discussion

The role of AQP5 in the regulation of lung fluid homeostasis and its potential contribution to lung function is largely unknown. In this study, we examined the expression pattern of AQP5 in mouse lung, and analyzed parameters of lung function in $Aqp5^{-/-}$ mice. The results presented here implicate a novel physiological role for AQP5 in cholinergic-stimulated bronchoconstriction.

Immunohistochemical analyses showed that AQP5 expression in mouse lung was not limited to type I cells, but was also detected in alveolar type II cells. Alveolar type II cells also express the epithelial sodium channel (ENaC), important in the transport of sodium across the alveolar epithelium (26, 27). Because water movement through AQPs is driven by osmotic gradients that are generated by sodium gradients, the coexpression of AQP5 and ENaC in alveolar type II cells may reflect coregulation of sodium and water transport in the alveolar region.

Physiological examination of $Aqp5^{-/-}$ mice by using resistance and compliance measurements and barometric whole body plethysmography showed that $Aqp5^{-/-}$ mice are hyperresponsive to bronchoconstriction by cholinergic stimulation. Our data suggest that the observed altered reactivity is not due to altered SP-B concentration. Thus, the mechanism of AQP5-mediated responsiveness is not likely to result in changes in surfactant-controlled surface tension. Other parameters of normal lung function were not affected by AQP5 deficiency. The absence of AQP5 expression did not affect gas exchange nor did it result in pulmonary edema under normal physiological conditions.

Identification of AQP5 expression in bronchial epithelial cells strongly implicates AQP5 as the previously described, but unidentified mercury-sensitive water channel responsible for mediating osmotically driven transcellular water flow and airway surface liquid composition (28, 29). It has been shown that a local increase in the osmolarity of the airway surface liquid as a result of respiratory water loss or inhalation of hypertonic saline induces bronchoconstriction in asthmatic patients (30, 31). Because bronchial epithelium has both metabolic and secretory functions that mediate both the release of bronchodilators and removal of bronchoconstricting agents (32–34), it is possible that the absence of AQP5 at the luminal surface of tracheal and bronchial epithelial cells leads to altered extracellular ionic composition that could affect the release and/or clearance of broncho-reactive substances, resulting in rapid airway responses. The lack of statistically significant alterations in smooth muscle contractility of trachea rings from $Aqp5^{+/+}$ and $Aqp5^{-/-}$ mice may be due to the fact that the immersion of the tracheal rings in a well-stirred PBS bath prevents changes in the local extracellular space. Alternatively, an AQP5-sensitive neural signaling pathway between the epithelium and smooth muscle may be disrupted in isolated tracheal ring preparations. Future studies by using methods that do not disrupt the integrity of the tracheal smooth muscle microenvironment will be needed to fully elucidate the mechanism responsible for the observed hyperreactivity.

Although our data clearly demonstrate a role for AQP5 in cholinergic-stimulated bronchoconstriction in mice, a "direct" role for AQP5 in this process has not yet been elucidated. Our data do not exclude the possibility that AQP5 ablation results in the aberrant expression of other developmentally regulated or physiologically relevant genes whose function may provide a direct mechanism for the enhanced bronchoresponsivenss that we observe in the *Aqp5* knockout mice. Additional analyses will be required to completely dissect the pathways involved in this AQP5-dependent response.

Sensitivity of bronchial airway smooth muscle to constriction by muscarinic agonists such as Ach or methacholine characterize both asthma and chronic obstructive pulmonary disease (COPD) in humans (33), pulmonary disorders that often are treated clinically with anticholinergic therapy (35, 36). Although the mechanism of its involvement is not known, these results indicate AQP5 involvement in a novel mechanism of bronchoconstriction.

Several genetic linkage studies have been conducted in both humans and mice to map the trait of airway hyperresponsiveness in asthma susceptibility. Of relevance to this report is a mouse quantitative trait locus (QTL) genetic mapping study performed by De Sanctis and colleagues (9). Airway hyperresponsiveness was mapped to mouse chromosome 15 (9) in the same region as the *Aqp5* gene locus (12). Two studies have mapped major asthma-susceptibility loci on human chromosome 12q (10, 11), the chromosomal location of human *Aqp5* gene (12). Human chromosome 12q and mouse chromosome 15 are syntenic within this region, which contains an aquaporin gene cluster (12, 13). None of the above linkage reports identify *Aqp5* as a candidate gene locus for asthma or bronchial hyperreactivity.

To our knowledge, there have been no previous reports showing a physiological role for AQP5 in modulating airway responsiveness and bronchoconstriction. The combined evidence presented by AQP5 lung expression patterns, physiological response to cholinergic challenge, and the colocalization of the *Aqp5* gene with chromosomal regions associated with airway hyperresponsive QTLs implicate this gene as a candidate for susceptibility to bronchial hyperreactivity and asthma.

We thank Drs. Stephen Liggett and Kevin Harrod for helpful discussions, and Maureen Luehrmann and Michelle Nieman for technical assistance. This work was supported by National Institutes of Health Grant RO1 DE138283 and National Institute of Environmental Health Sciences Grant ES 06096 (A.G.M.) and the National Heart Lung and Blood Institute Program of Excellence in Molecular Biology of Heart and Lung Grants HL61781 (to A.G.M. and for support of C.M.K. as a New Investigator in this program) and HL56387, and the Cystic Fibrosis Foundation (to J.A.W. and S.E.W.).

1. Raina, S., Preston, G. M., Guggino, W.B. & Agre, P. (1995) *J. Biol. Chem.* **270,** 1908–1912.
2. Nielson, S., King, L. S., Christensen, B. M. & Agre, P. (1997) *Am. J. Physiol.* **273,** C1549–C1561.
3. King, L. S., Nielsen, S. & Agre, P. (1997) *Am. J. Physiol.* **273,** C1541–C1548.
4. Towne, J. E., Harrod, K. S., Krane, C. M. & Menon, A. G. (2000) *Am. J. Respir. Cell Mol. Biol.* **22,** 34–44.
5. Towne, J. E., Krane, C. M., Bachurski, C. J. & Menon, A. G. (2001) *J. Biol. Chem.* **276,** 18657–18664.
6. Borok, Z., Lubman, R. L., Danto, S. L., Zhang, X. L., Zabski, S. M., King, L. S., Lee, D. M., Agre, P. & Crandall, E. D. (1998) *Am. J. Respir. Cell Mol. Biol.* **18,** 554–561.
7. Ma, T., Fukuda, N., Song, Y., Matthay, M. A. & Verkman, A. S. (2000) *J. Clin. Invest.* **105,** 93–100.
8. Song, Y., Fukuda, N., Bai, C., Ma, T., Matthay, M. A. & Verkman, A. S. (2000) *J. Physiol.* **525,** 771–779.
9. De Sanctis, G. T., Merchant, M., Beier, D. R., Dredge, R. D., Grobholz, J. K., Martin, T. R., Lander, E. S. & Drazen, J. M. (1995) *Nat. Genet.* **11,** 150–154.
10. Malerba, G., Lauciello, M. C., Scherpbier, T., Trabetti, E., Galavotti, R., Cusin, V., Pescollderungg, L., Zanoni, G., Martinati, L. C., Boner, A. L., *et al*. (2000) *Am. J. Respir. Crit. Care Med.* **162,** 1587–1590.
11. Wjst, M., Fischer, G., Immervoll, T., Jung, M., Saar, K., Rueschendorf, F., Reis, A., Ulbrecht, M., Gomolka, M., Weiss, E. H., *et al*. (1999) *Genomics* **58,** 1–8.
12. Lee, M. D., Bhakta, K. Y., Raina, S., Yonescu, R., Griffin, C. A., Copeland, N. G., Gilbert, D. J., Jenkins, N. A., Preston, G. M. & Agre, P. (1996) *J. Biol. Chem.* **271,** 8599–8604.
13. Krane, C. M., Towne, J. E. & Menon, A. G. (1999) *Mamm. Gen.* **10,** 498–505.
14. Krane, C. M., Melvin, J. E., Nguyen, H. V., Richardson, L., Towne, J. E., Doetschman, T. & Menon, A. G. (2001) *J. Biol. Chem.* **276,** 23413–23420.
15. Hand, A. R. (1995) in *Introduction to Biophysical Methods for Protein and Nucleic Acid Research*, eds. Glasel, J. A. & Deutscher, M. (Academic, New York), pp.205–260.
16. Yang, B., Norimasa, F., van Hoek, A., Matthay, M. A., Ma, T. & Verkman, A. S. (2000*) J. Biol. Chem.* **275,** 2686–2692.
17. Gavett, S. H., Madison, S. L., Stevens, M. A. & Costa, D. L. (1999) *Am. J. Respir. Crit. Care Med.* **160,** 1897–1904.
18. Ewart, S., Levitt, R. & Mitzner, W. J. (1995) *Appl. Physiol.* **79,** 560–566.
19. Hamelmann, E., Schwarze, J., Takeda, K., Oshiba, A., Larsen, G. L., Irvin, C. G. & Gelfand, E. W. (1997) *Am. J. Respir. Crit. Care Med.* **156,** 766–775.
20. McGraw, D. W., Forbes, S. L., Kramer, L. A., Witte, D. P., Fortner, C. N., Paul, R. J. & Liggett, S. B. (1999) *J. Biol. Chem.* **274,** 32241–32247.
21. Kao, J., Fortner, C. N., Liu, L. H., Shull, G. E. & Paul, R. J. (1999) *Am. J. Physiol.* **277,** L264–L270.
22. Tokieda, K., Iwasmoto, H. S., Bachurski, C., Wert, S. E., Hull, W. M., Ikeda, K. & Whitsett, J. A. (1999) *Am. J. Respir. Cell Mol. Biol.* **21,** 463–472.
23. Kreda, S. M., Gynn, M. C., Fenstermacher, D. A., Boucher, R. C. & Gabriel, S. E. (2001) *Am. J. Respir. Cell Mol. Biol.* **24,** 224–234.
24. Glaser, S. W., Korfagen, T. R., Weaver, T. E., Pilot-Matias, T., Fox, J. L. & Whitsett, J. A. (1987) *Proc. Natl. Acad. Sci. USA* **84,** 4007–4011.
25. Tokieda, K., Whitsett, J. A., Clark, J. C., Weaver, T. E., Ikeda, K., McConnell, K. B., Jobe, A. H., Ikegami, M. & Iwamoto, H. S. (1997) *Am. J. Physiol.* **273,** L875–L882.
26. Hummeler, E., Barker, P., Gatzy, J., Beerman, F., Verdumo, C., Schmidt, A., Bocher, R. & Rossier, B. C. (1996) *Nat. Genet.* **12,** 325–328.
27. Matalon, S., Benos, D. J. & Jackson, R. M. (1996) *Am. J. Physiol.* **271,** L1–L22.
28. Willumsen, N. J., Davis, C. W. & Boucher, R. C. (1994) *J. Clin. Invest.* **94,** 779–787.
29. Matsui, H., Davis, C. W., Tarran, R. & Boucher, R. C. (2000) *J. Clin. Invest.* **105,** 1419–1427.
30. Anderson, S. D. (1998) in *Asthma: Basic Mechanisms and Clinical Management,* eds. Barnes, P. J., Rodger, I. W. & Thomson, N. C. (Academic, New York), pp. 569–587.
31. Anderson, S. D., Schoeffel, R. E. & Finney, M. (1983) *Thorax* **38,** 284–291.
32. Boucher, R. C. (1994) *Am. J. Respir. Crit. Care Med.* **150,** 581–593.
33. Hegele, R. G., Hayashi, S., Hogg, J. C. & Pare, P. D. (1995) *Am. J. Respir. Crit. Care Med.* **151,** 1659–1665.
34. Folkerts, G. & Nijkamp F.P. (1998) *Trends Pharmacol. Sci.* **19,** 334–341.
35. Campbell, S. C. (2000) *Respir. Care* **45,** 864–867.
36. Manning, H. L. (2000) *Curr. Opin. Pulm. Med.* **6,** 99–103.